

Dan André Johansen

A Coupled Battery Production and Life Cycle Inventory (LCI) model

Master's thesis in Energy and Environmental Engineering

Supervisor: Anders Hammer Strømman

Co-supervisor: Asanthi Jinasena, Lorenzo Usai, Odne Stokke Burheim

July 2021

Dan André Johansen

A Coupled Battery Production and Life Cycle Inventory (LCI) model

Master's thesis in Energy and Environmental Engineering
Supervisor: Anders Hammer Strømman
Co-supervisor: Asanthi Jinasena, Lorenzo Usai, Odne Stokke Burheim
July 2021

Norwegian University of Science and Technology
Faculty of Engineering
Department of Energy and Process Engineering



Preface

This thesis is the final chapter of my MSc in Energy and Environmental Engineering, carried out at the Norwegian University of Science and Technology in the spring of 2021.

I want to thank my supervisor Anders Hammer Strømman, and my co-supervisors Asanthi Jinasena and Lorenzo Usai for their excellent guidance during this process. A special thanks goes to my co-supervisors for all their advice and tireless support throughout this project, both day and night. You have been invaluable through the ups and downs of the project, the data wrangling, programming and writing that has resulted in 3.000 lines of code, this thesis and a ton of lessons learnt.

And for my girlfriend. There are no words that can describe my gratitude for the tremendous patience you have shown, the countless advice you have given in times of need, and all the motivation you have given me during the writing of this thesis, and in life in general. From the bottom of my heart -- Thank you!

Dan André Johansen

Abstract

In order to meet the ever more inevitable challenges of climate change, the global transportation sector will need to undergo great changes in the following decades. Electrification of road vehicles is seen as an essential part of the solution, with battery technology being a key enabler of the shift towards a more sustainable transport sector. Following ambitious mitigation policies and technological advancements, the number of electrical vehicles on the road has grown rapidly over the last decade and is predicted to accelerate its steep growth over the next decade. This development requires an increase of battery production capacity and a focus on the energy usage and emissions from the manufacturing process.

To avoid problem-shifting and to foster robust decisions on how production processes can be designed and improved, a life cycle perspective is needed, as well as the resolution, uncertainty and variance management that engineering models can bring to the table. The aim of this thesis is thus to combine the research strands of Life Cycle Assessment (LCA) and process modeling into a coupled battery production and Life Cycle Inventory (LCI) model. The development, hereunder programming, of this coupled model make up the largest part of the thesis work.

The coupled model consists of a Python (3.9.2) based interface which connects an LCA model with a Python (3.7) based cell production model. A generalized and flexible battery production process model developed by Jinasena et al. (2021) has been coupled with the LCI of Ellingsen et al. (2014) for the materials and energy use for lithium-ion battery (LiB) manufacturing. The

resulting coupled model can semi-automatically incorporate the production information of battery production into the LCI for various input requirements.

The Python interface thus eliminates the user's need to use Microsoft Excel to structure the LCI, and allows the possibility of running multiple scenarios in a much more streamlined way. This approach has the potential to significantly reduce both the workload and time required to go from battery production data on energy and material consumption to a complete LCA. In addition, the flexibility of the program would allow the LCA to be adjusted and applied for several other products and services.

Sammendrag

I et forsøk på å overkomme de stadig mer uunngåelige utfordringene som følge av klimaforandringene, må den globale transportsektoren gjennomgå store endringer de neste tiårene. Elektrifisering av kjøretøy blir sett på som en essensiell del av løsningen, hvor batteriteknologi spiller en sentral rolle i overgangen til en mer bærekraftig transportsektor. Ved hjelp av en ambisiøs politikk og teknologiske fremskritt har antallet elektriske kjøretøy på veiene økt betraktelig i løpet av det siste tiåret, og er forventet å øke i et enda raskere tempo over det neste tiåret. Denne utviklingen krever en økning av batteriproduksjonskapasiteten, og et fokus på energiforbruk og utslipp fra produksjonsprosessen.

For å unngå å en problemforskyvning og for å fatte robuste vedtak for utviklingen og forbedringen av produksjonsprosesser, må man ha et livssyklusperspektiv, i tillegg til detaljnivået og usikkerhets- og endringshåndteringen man kan få ved å introdusere engineering-modeller. Målet med denne oppgaven er derfor å kombinere forskningsstrømmene i livssyklusanalyse og prosessmodellering til en sammenkoblet produksjons- og livssyklusinventarmodell. Utviklingen, herunder programmeringen, av den sammenkoblede modellen, utgjør den største delen av dette masterprosjektet.

Den sammenkoblede modellen består av et Python (3.9.2)-basert grensesnitt, som kobler sammen en livssyklusmodell med en Python (3.7)-basert celleproduksjonsmodell. En generalisert og fleksibel batteriproduksjonsprosessmodell utviklet av Jinasena et al. (2021) har blitt koblet sammen med livssyklusinventaret fra Ellingsen et al. (2014) for material- og energiforbruket for å produsere litium-ion-batteri. Den sammenkoblede modellen kan delvis

automatisk inkorporere produksjonsinformasjonen for batteriproduksjonen i livssyklusinventaret, basert på forskjellige kriterier.

Python-grensesnittet eliminerer dermed brukerens behov for å bruke Microsoft Excel og for å strukturere livssyklusinventaret, og gjør at man kan kjøre flere ulike scenarioer mye mer strømlinjeformet. Denne fremgangsmåten har muligheten til å vesentlig redusere både arbeidsmengden og tidsbruken som er nødvendig for å gå fra å ha data på energi- og materialforbruk for batteriproduksjonen, til å ha en ferdig livssyklusanalyse. I tillegg kan programmets fleksibilitet gjøre at man kan tilpasse og bruke livssyklusanalyse for andre produkt og tjenester.

Table of contents

Preface	1
Abstract	i
Sammendrag	iii
List of figures	vi
List of tables	vi
List of abbreviations	vii
1 Introduction	1
1.1 Background.....	1
1.2 Literature review	2
1.3 Objective of the thesis.....	4
2 Battery production and modelling	6
2.1 Battery production	6
2.2 Battery production modelling	9
3 LCA and methodological framework	12
3.1 Life Cycle Assessment.....	12
3.1.1 <i>General introduction of the field</i>	12
3.1.2 <i>Four stages of LCA</i>	12
3.1.3 <i>Mathematical framework</i>	15
3.2 The benefits and need for linking LCA and engineering models	17
4 Model development	20
4.1 Synthesis of needs, objectives and requirements	20
4.2 Presentation of the coupled model.....	21
4.3 Software	29
4.4 Development of the coupled model.....	30
4.5 Model example applications	33
5 Limitations and further work	37
5.1 Limitations.....	37
5.2 Further work.....	37
References	38

List of figures

Figure 1 A block diagram of a generalized battery cell production line (Jinasena et al., 2021).
..... 6

Figure 2 A four-stage convection heat oven for electrode drying (Bryntesen et al., 2021). .. 7

Figure 3 Three ways to stack or wind the electrodes and separator (Schmitt et al., 2014).. 8

Figure 4 Illustration of the model system structure as applied in Jinasena et al. (2021),
showing the selected battery production process steps and model structure, including
the main inputs, outputs and the main units (figure from Jinasena et al., 2021, p. 13). 10

Figure 5 The four stages of an LCA (Ouellet-Plamondon & Habert, 2015) 13

Figure 6 Coupled battery production and LCI model. The production model is adapted from
Jinasena et al. (2021), while the LCI model is based upon a generic template. 22

Figure 7 Comparison of example data for GHG emissions from the coupled model with
reference data from litterature 34

List of tables

Table 1 The ten different combinations of cathode and anode active materials modelled by
the process model, of which seven are active in the CBPLM. Inactive combinations are
marked with an asterix. 24

Table 2 Overview of the cell components contained in the dataset. 25

Table 3 Process steps accounted for in the LCI (right side) and the associated main
components (left side). 26

Table 4 Breakdown of CO2 emissions due to the cell materials 35

Table 5 Breakdown of CO2 emissions due to the direct energy use of the cell production
processes 36

List of abbreviations

BEV = Battery electric vehicle

CMC = Carboxymethyl Cellulose (binder material, anode and cathode)

CBPLM = The Coupled Battery Production and LCI Model presented in this thesis

EV = Electric vehicle

GHG = Greenhouse gases

GWP = Global warming potential

LCA = Life cycle assessment

LCI = Life cycle inventory

LCIA = Life Cycle Impact Assessment

LFP = Lithium-iron-phosphate (cathode material)

LIB = Lithium-ion battery

LiFP6 = Lithium hexafluorophosphate (electrolyte material)

LMO = Lithium manganese oxide (cathode material)

LTO = Lithium titanate oxide (anode material)

NCA = Lithium nickel cobalt aluminum oxide (cathode material)

NMC = Lithium nickel manganese cobalt oxides (cathode material)

NMP = N-methyl pyrrolidone (solvent material, anode)

Plastic PP = Plastic polypropylene (pouch cell container material)

Plastic PET = Plastic Polyethylene terephthalate (pouch cell container material)

PVDF = Polyvinylidene fluoride (binder material, anode and cathode)

SBR = Styrene-butadiene rubber (binder material, anode and cathode)

Si = Silicon (anode material)

1 Introduction

1.1 Background

As the threats of climate change become more manifest in terms of both natural disasters and policy measures, the transport sector enters a critical phase. Transportation is responsible for about 24% of direct CO₂ emissions from fuel combustion globally, with road vehicles accounting for nearly three-quarters of the emissions (IEA, 2020c). The International Energy Agency has estimated that the transportation sector has the potential to reduce 18% of global greenhouse gas emissions by 2050 (IEA, 2019, as cited by Cerdas, 2020). and electrification of vehicles is seen to play a key role in the transition to a more sustainable transport sector. Entering commercial markets around 2010, the number of electrical vehicles (EVs) on the road has rapidly grown (IEA, 2020b). And the electrification of the transport sector is not expected to slow down soon, rather, the number of EVs is predicted to increase with more than 30 times of today's amount by 2030 (ibid), and electrification of vehicles is seen to play a key role in the transition to a more sustainable transport sector. Entering commercial markets around 2010, the number of electrical vehicles (EVs) on the road has rapidly grown (IEA, 2020b). And the electrification of the transport sector is not expected to slow down soon, rather, the number of EVs is predicted to increase with more than 30 times of today's amount by 2030 (ibid).

Electrifying the transport sector poses several challenges which needs to be addressed, avoiding emission-related problem shifting being one of them. For example, while EVs have no tailpipe emissions, the production phase exhibits higher Global Warming Potential (GWP) impacts than conventional vehicles

(Hawkins et al., 2013). Thus, when analyzing the environmental trade-offs of changing from conventional, fossil-fuel vehicles to EVs, a life cycle perspective is needed (Ellingsen et al., 2017), and life cycle assessment (LCA) is a fruitful approach herein (Nealer & Hendrickson, 2015). LCA also has the potential of providing environmental insights that can be valuable in improving EV production processes generally and for battery production processes more specifically (Cerdas, 2020).

1.2 Literature review

Following the rapid growth of global use of EVs, a considerable amount of LCAs of EV batteries have been performed over the past decade. Studies have estimated the battery system of EVs to account for 35–44% of the GWP caused during the production stage (Volkswagen, 2012; Hawkins et al., 2013; Ellingsen et al., 2014; Dunn et al., 2015; Cerdas, Titscher, et al., 2018; as cited by Cerdas, 2020). Lithium-ion batteries are the most prevalent among EV batteries today, and is expected to dominate the EV battery market for the next decade (IEA, 2020a).

However, there are several limitations in the current studies, which results in considerable disparities in the estimated GWP from EV battery production processes. Some of the biggest challenges is access to data; current LCA methodologies' ineptness in dealing with the highly complex nature of battery production processes; and trade-offs between quality and resource-use of current practices, especially in the industry.

Therefore, existing LCA studies of the production of lithium-ion batteries show a high variance of GWP emissions. Within what can be characterized as the main base studies of the field, the results range from 1,1 to 424 kg CO₂-eq

per kWh (Jinasena, 2021), the two extremes being Notter et al. (2010) estimating 1,14 kg CO₂-eq/kWh in their study on Lithium-ion Manganese Oxide (LMO) batteries for Battery Electric Vehicles (BEV), and Ellingsen et al. (2014) suggesting a range of 107–424 kg CO₂-eq/kWh for Nickel Manganese Cobalt (NMO) BEV batteries. When reviewing recent LCA and modeling studies on lithium-ion battery production, Jinasena et al. (2021) find high variances between the studies' reported battery manufacturing energy, both in terms of energy usage; percentage of total GWP emissions, and battery GWP, despite the fact that the LCA inventory values were based on the same set of base studies. The widely different results stem from the fact that most studies use general data for battery production systems that differ fundamentally, e.g., in terms of location of the battery production factory; and the type, energy and chemistry of the battery cells being produced (Jinasena, 2021).

There are, however, some studies that report on energy consumption for different process steps by using primary data from actual battery production plants (Schünemann, 2015; Pettinger & Dong, 2016; Yuan et al., 2017; Dai et al., 2019; Thomitzek et al., 2019; Sun et al., 2020). Summarizing the overall findings of these studies, Jinasena et al. (2021) argues that these data generally show that energy usage decreases when the plant capacity increases. Moreover, the authors argue that difference between these data and data from the above-mentioned LCA studies probably results from the fact that mass production plants optimize for profit and lowering energy usage, while pilot scale plant facilities that are designed for research optimize for product quality.

In order to deal with such variations and allow for effectively comparing of different production options (e.g., for different cell material and chemistry options), there is a need for process models that are flexible to key factors of general production processes (Jinasena, 2021).

To date, few modeling studies have been conducted, and for the most part, these are developed for individual process steps, and mostly focused on quality parameters and performance, neglecting the GWP of the process (see for example Meyer et al., 2018; Schreiner et al., 2019; Mayer et al., 2020). The limited numbers of studies presenting model structures of material and energy flow modeling (see for example Herrmann & Thiede, 2009; Schönemann et al., 2019) are inadequate to use for general cases and not possible to integrate with LCA models (Jinasena, 2021).

A promising exception from these limitations, is the multi-level modeling approach of Thomitzek et al. (2018) which can be used to predict the impact of different distributions of product and process parameter deviations in battery production processes. Building upon the work of Thomitzek et al. (2018), Jinasena et al. (2021) introduces an industrial scale process model that determines the material and energy flows of a general lithium-ion battery cell manufacturing, which is flexible for different battery chemistries, types, throughputs and process technologies, and which allows for integration with LCA models.

1.3 Objective of the thesis

Drawing upon the research strand of LCA on one hand, and process modeling on the other hand, this aim of the study at hand is to couple these approaches

to create a model that semi-automatically produces LCIs based upon inputs from a battery-production process model and a set of user choices.

The goal is to make use of the process model made by Jinasena et al. (2021) and convert the output of such process models into a format that can be useful in the context of LCA. Process models often do not keep track of production aspects of relevance for LCA, such as composition of electrolytes (i.e., how much material is used in 100g of electrolytes). Moreover, part of the work is to convert the list of material composition and energy consumption from Jinasena et al. (2021) into a matrix form that is in the right format for LCA, and matching the materials with the background processes.

The thesis is structured in the following way: Chapter 2 provides an overview of relevant EV battery production processes and the engineering modeling approach the thesis builds upon. In chapter 3, the methodological framework LCA is presented. Here, a general introduction to LCA is given before the argument is made that bridging LCA and engineering models may yield several benefits for considering energy use and GHG emissions from EV battery production. Then, the development of the coupled model is described in chapter 4. First, the needs, objectives and requirements of the model is synthesized, before the model in itself is presented. Utilized software and the programming process are also described in this chapter, before moving on to an example application of the model. Chapter 5 concludes the thesis by summarizing the work and the capabilities of the model, as well as limitations and venues for further work.

2 Battery production and modelling

This chapter provides an overview of battery production processes of relevance to this thesis and briefly describes battery production modelling.

2.1 Battery production

The production of a battery cell contains a lot of steps, some of which are dependent on the type of battery, e.g., if it is a prismatic cell, coin cell, or a cylindrical cell. In this chapter, a generalized production chain is shown and the necessary steps can sometimes be dependent on the type of battery cell. As shown in Figure 1, the battery cell production process chain can be divided into three main phases, namely electrode manufacturing, cell assembly, and cell finishing. This is a somewhat aggregated version, as a real battery production process usually can be divided into even more separate processes.

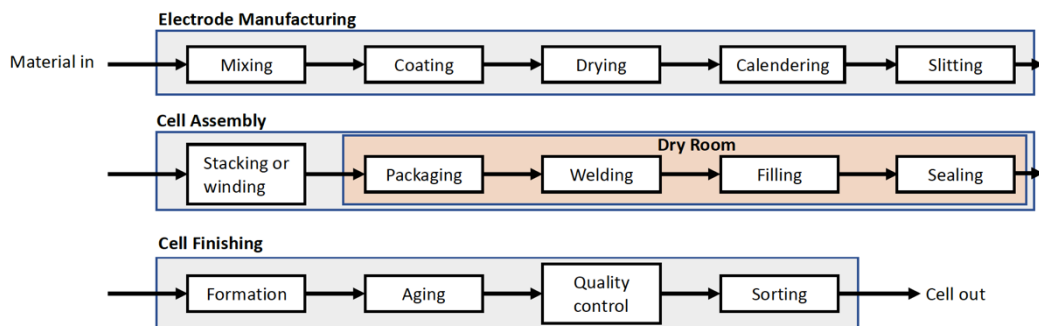


Figure 1 A block diagram of a generalized battery cell production line (Jinasena et al., 2021).

The first phase, electrode manufacturing, starts off with mixing the active material, solvent, binders, and conductive additives together to a slurry. This slurry is then coated on to thin metal sheets called current collectors. The material commonly used for the current collectors are copper for the negative

electrode and aluminum for the positive electrode. In the next step, the coated electrodes are dried by being fed through special ovens with different temperature zones, as shown in Figure 2. This is to adhere the coating to the current collectors in a controlled fashion, while achieving a middle ground between mechanical strength and flexibility. In addition, the solvent used in the slurry is removed from the coating during this step. When the coating is fixed, the now coated current collectors are calendered to compress the coating layer to carefully calculated densities. This phase ends by the slitting process, where the electrodes are slitted to their correct width.

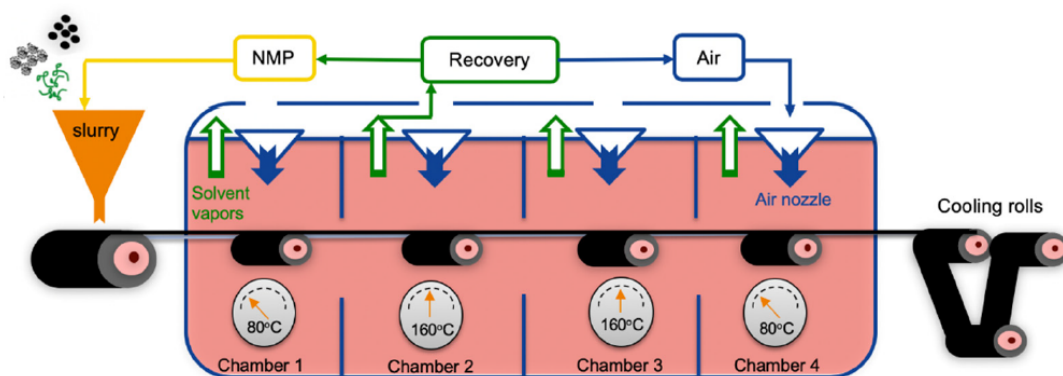


Figure 2 A four-stage convection heat oven for electrode drying (Bryntesen et al., 2021).

In the second phase, which is the cell assembly phase, the first step is to make a winding if it is a prismatic, cylindrical or coin cell, or a stack if it is a pouch cell. This winding or stack contains several layers of the current collectors and a separator. This is done by alternating the type of current collector, while always having a separator between the current collectors, as can be seen in Figure 3. The two pictures on the left shows how the separator, represented by the white sheets or roll depending on if it is discrete sheets or a continuous roll of the separator material, is placed between the anode and cathode. The anode

is represented by the sheets of one shade of grey, while the cathode is represented by the sheets of the other shade of grey. In the bottom-left picture, one can see how the electrodes and the separator can be wound, with both electrodes and the separator material being continuous rolls of material. The materials shown in the picture are, from top to bottom, an anode (or cathode), a separator, a cathode (or anode), and finally another separator.

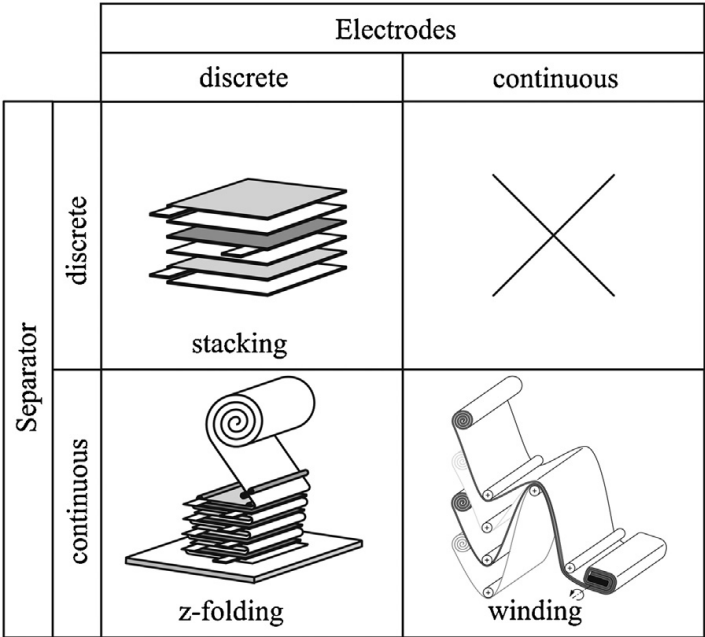


Figure 3 Three ways to stack or wind the electrodes and separator (Schmitt et al., 2014).

When the stacking process is complete, the stacks are packed in pouches, connector tabs in the same material as the respective current collectors are welded on to the end of the current collectors, before the cell is filled with electrolyte and sealed shut. The stacking, welding, filling and sealing process steps are all taking place inside a dry room e.g., to avoid moisture from reacting with the electrolyte, which would rend it unusable.

The final phase is the cell finishing, where it starts off by formation of the cell. That is, the cell is charged and discharged several times to produce the solid-electrolyte interface (SEI) layer on the anode, which prevents it from degrading further as it limits the liquid contact between the electrolyte and the anode. The final three steps of the production-process chain are the ageing, quality control and sorting. For the ageing process step, the cell is stored away for some weeks time to see how it degrades over time. The quality control and sorting are where they measure various cell parameters and removes the ones that don't pass the control and puts the rest into different categories based on their performance.

2.2 Battery production modelling

When incorporated into LCA models, process modelling can provide specific material and energy values to LCA studies on battery manufacturing; deal with the variations and uncertainties inherent in the manufacturing process; and allow for comparison of different production options (Jinasena et al., 2021). As described in the brief literature review in the introduction chapter of this thesis, there exists a few modeling studies looking at the energy flow and connected GWP of the battery manufacturing processes, but most of them are limited by scope (as they focus on individual process steps) and inaptness for integration with LCA models (see chapter 1).

In this thesis, I build upon the battery production process model developed by Jinasena et al. (2021). Their process model calculates energy and material demands for different battery types, plant capacities, and process steps. Validating the results of the model using existing literature values, Jinasena et al. (2021) finds their process model to be comparable with studies of gigascale factories (Kurland, 2019; Sun et al., 2020). Note that the model is not

validated using industrial data; this could, as Jinasena et al. (2021) argue, have further enhanced the model's accuracy. Because this model is flexible, includes material and energy flows and process steps for different cell types and chemistries, and is focused on industrial-scale plants (in contrast to the smaller pilot plants which oftentimes are used in research), it seems like a fruitful starting point for the study at hand. The rest of this sub-chapter provides an overview of the process model of Jinasena et al. (2021). The flexible model system structure which is applied in the process model, is shown in Figure 4.

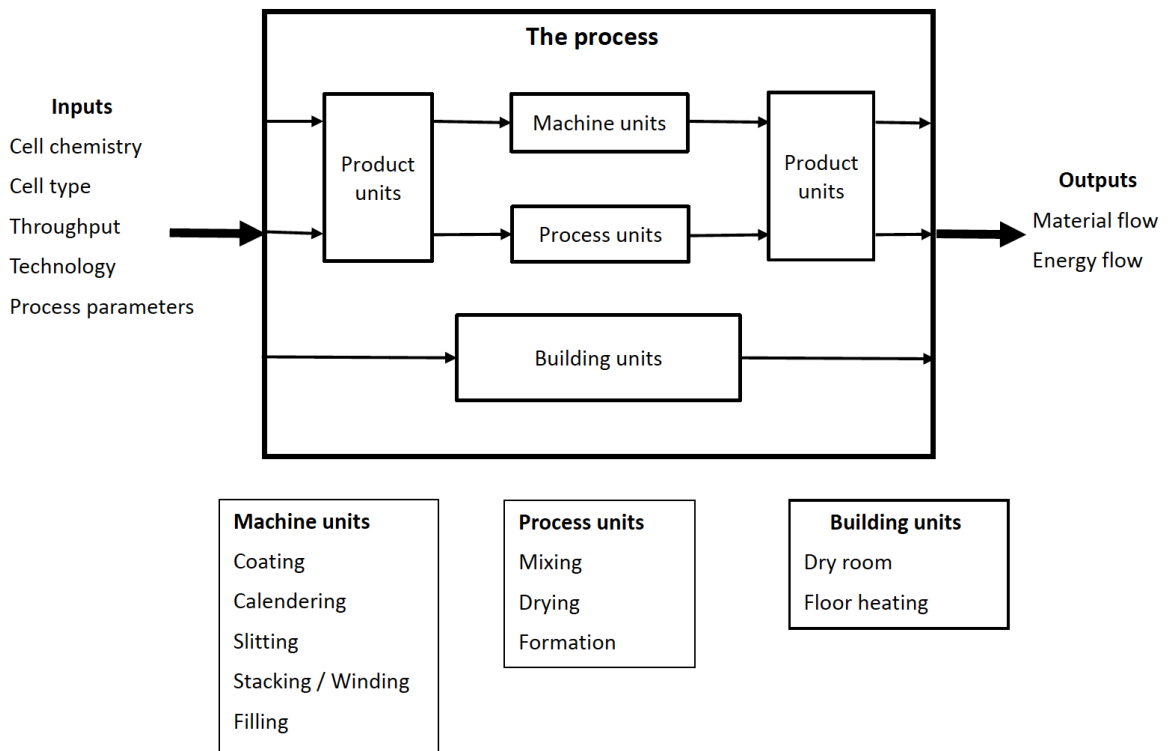


Figure 4 Illustration of the model system structure as applied in Jinasena et al. (2021), showing the selected battery production process steps and model structure, including the main inputs, outputs and the main units (figure from Jinasena et al., 2021, p. 13).

The variable inputs to the model include the cell chemistry, yielding a selection of ten different combinations of cathode and anode chemistries, which can be found in table x tk. Further, it gives the option to choose between the three different cell types: pouch, prismatic and cylindrical. The third input variable is the throughput, which lets the user vary the amount of annual throughput for the simulated production plant. The two final inputs let the user change the type of technology to consider and process parameters for selected process steps. The two inputs yield information about the material masses that goes into a process, how much of it that comes out of it, and the energy usage for each of the energy consuming processes.

The model contains four main types of units. The first one is the product units, which keeps track of the initial, intermediate, and final material masses at each process step for components such as the active material, binder, electrolyte, separator, and carbon black. The second one is the machine units, which modifies the simulated specifications for the machinery in the production line, based upon commercially available information and the chosen throughput of cells to be simulated, by using engineering calculations. The process units monitor the energy consumption for some of the most energy intensive or cell-quality influential processes in the production, by using physical principles that have been simplified. The final type is the building units. These types of units cover the energy use for the dry room and floor heating, using engineering calculations to account for several parameters such as the ambient air temperature, the total heating load, the floor heating area, and parameters to idling time of the machines and machine efficiencies.

3 LCA and methodological framework

The first part of the chapter provides a general introduction to the field of life cycle assessment, how LCA is commonly divided into four stages, and finally an overview of the mathematical framework for LCA. The second part of the chapter highlights some of the advantages and need to link LCA models to engineering models together.

3.1 Life Cycle Assessment

In this subchapter, the Life Cycle Assessment (LCA) framework is introduced by a brief explanation of what LCA is, the stages of an LCA, and the mathematical framework of LCA. This subchapter is to a large extent based upon my own previous description of LCA in Johansen (2020).

3.1.1 General introduction of the field

Life Cycle Assessment (LCA) is a method used to assess the environmental impacts for a product due to the material and energy use related to the product, through parts of or the entire life cycle, where the entire life cycle is usually from resource extraction to disposal or recycling of the product (The International Standards Organisation, 2006). The system boundaries of this project's LCA is cradle-to-gate, meaning that it starts at the extraction of the materials used (cradle) and ends at a complete product (gate), which in this thesis will be a battery cell.

3.1.2 Four stages of LCA

There are commonly four stages to an LCA, namely Goal and scope definition, Inventory analysis or Life Cycle Inventory (LCI), Impact Assessment (LCIA), and Interpretation, as visualized in Figure 5.

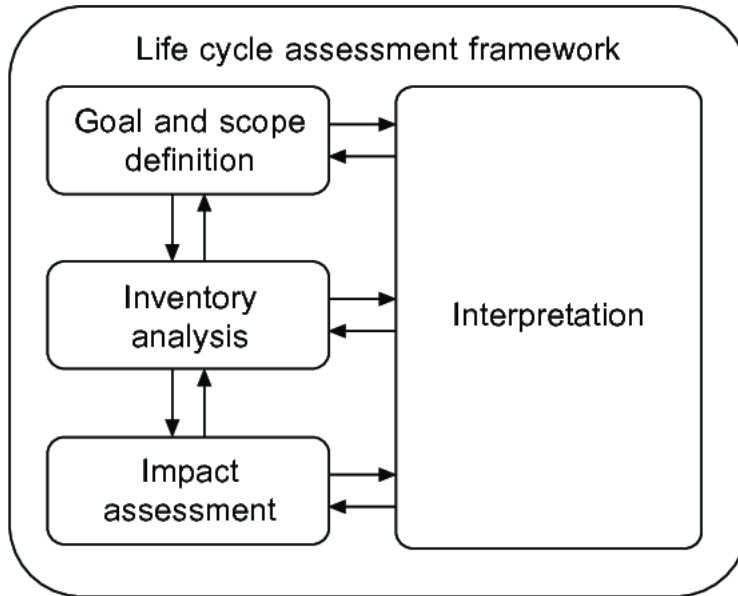


Figure 5 The four stages of an LCA (Ouellet-Plamondon & Habert, 2015)

(1) Goal and scope definition

The goal and scope definition cover, among other, which product and which environmental impact types to be investigated, the system boundaries, and the functional unit of the analysis, where the functional unit is a reference unit which allows for comparison between similar products i.e., 1 electric bike, 150 000 km/year driven by a vehicle, per unit of battery cell, per kg of product, etc.

(2) Life Cycle Inventory

In the Life Cycle Inventory (LCI) stage, the activities associated with the processes within the system boundaries are mapped to get all the quantitative data which e.g., can be the emissions, energy and/or material flows, and much more. Once all the relevant data have been gathered, it must be systematized to find the various stressors, which is a term used in LCA terminology to

describe the emissions, waste, use of resources, etc., such as the number of CO₂-equivalents emitted. This can be done e.g., by matrix algebra, as explained below, or by an LCA software, such as the Arda tool, which is an LCA software developed at NTNU. This stage is the focal point of this thesis.

(3) Life Cycle Impact Assessment

At the third stage, where the Life Cycle Impact Assessment (LCIA) is performed, the stressors are converted into comparable and more intuitive impact types, such as Global Warming Potential (GWP), using characterization factors. Characterization factors are values in terms of how much a stressor contributes to an impact, i.e., for GWP, which is commonly calculated in CO₂-equivalents, CO₂ has a value of 1 kg CO₂-eq./kg CO₂, CH₄ a value of 34 kg CO₂-eq./kg CH₄, and N₂O a value of 298 kg CO₂-eq./kg N₂O, to mention some. It is also possible to extend this further to a midpoint level or endpoint level using the ReCiPe method, which for the endpoint level is to attempt to say something about the effects these stressors could have on e.g., ecosystem damage, human health, etc., but these impact categories become more abstract, and thus less accurate, the further they are extended from the basic impact level.

(4) Interpretation

Finally, we have the Interpretation stage. At this stage, the results are processed to draw conclusions and to make them more readily presentable to an audience. Uncertainties, critical assumptions and so forth, of the study should be identified at this stage. However, this stage runs alongside the three previous steps as an integral part of them throughout the entire LCA. This is a part of LCA which cannot be automated: it is up to the practitioner to find relevant outcomes and interpret results.

3.1.3 Mathematical framework

The LCA framework is mathematically operationalized by using a matrix notation structure. The primary matrices and vectors utilized in LCA are briefly presented in the following sections.

The requirements matrix, represented by A , consists of a foreground and a background system. The foreground system is the processes defined in individual studies, while the background system consists of processes from a generic database. In addition, the values in the A matrix describes the interdependencies of the various processes. The y vector is a vector that describes the final demand of a LCA production process, and which is commonly the same as the functional unit described in the goal and scope definition. A total output vector, represented by x , can be calculated from the identity matrix I , the requirements matrix A , and the final demand vector y , using equation (1) below.

$$(1) x = (I - A)^{-1} * y$$

$A = requirements\ matrix$

$y = final\ demand = functional\ unit$

$x = total\ output\ vector$

$I = identity\ matrix$

Mathematically, the equation is calculated and rearranged as follows:

$$x = A * x + y \rightarrow x - A * x = y \rightarrow x * (I - A) = y \rightarrow x = (I - A)^{-1} * y$$

The C matrix is filled with characterization factors, which helps us convert different stressors into equivalent units i.e., CO₂-equivalents, making it possible to compare and sum up the impacts caused by different stressors causing the same type of impact. S is the stressor intensity matrix and is defined as the intensity of a stressor per unit of output of a given process. By performing a contribution analysis, one can show where an impact stem from. To do this, one would calculate the D_{pro} matrix by using a diagonalized x matrix, denoted as \hat{x} , along with the C and S matrices which can be combined as shown in equation (2).

$$(2) D_{\text{pro}} = C * S * \hat{x}$$

C = characterization matrix

S = stressor intensity matrix

D_{pro} = contribution analysis (impacts from different processes)

To find the total impacts for each category, one can calculate the d vector, as shown in equation (3).

$$(3) d = C * S * x$$

*d = C * x = total impacts vector*

Summing each of the rows of the D_{pro} matrix will also yield the d vector.

3.2 The benefits and need for linking LCA and engineering models

Although LCA can be applied to engineering activities such as product development (Hauschild et al., 2013), various features inherent in LCA methodology have thus far hindered the framework from becoming a mainstream engineering tool (Cerdas, Thiede, et al., 2018). Current LCA methodologies and tools are unable to adequately cope with the increasing complexity of electrical vehicles and their components, thus hindering LCA's usefulness in considering mitigation options within decision-making and product development in the sector (Cerdas, 2020). More specifically, issues arise from current LCA practices being assessment-oriented; reliant on high degrees of expert knowledge; and resource-intensive.

Traditional LCA is, as the term implies, assessment oriented, with analyses resulting in concrete values (e.g. stating the CO₂-eq of a process), hence overlooking the variability and uncertainty of the process at hand. Here lies a significantly beneficial potential of coupling LCA with engineering models, Cerdas (2020) argues:

(...) if engineers change the focus from an assessment-oriented application (resulting, for instance, in a value e.g. 120 g CO₂-eq/km) to a variability and uncertainty oriented application (resulting in a model, a range, a constraint, etc.), more reliable solutions can be developed, and better optimization strategies can be found. This is perhaps one of the most significant benefits of embedding LCA and its scientific foundation within engineering activities. (Cerdas, 2020, p. 12–13)

Moreover, the LCA approach allows for a wide range of different modelling choices that may affect the result considerably, and therefore demands high

degrees of expert knowledge (Hauschild et al., 2018). The modelling freedom of LCA enables companies to make – knowingly or un-knowingly – misleading environmental claims about a system while arguing that they have applied scientific methodology (Cerdas, 2020). On a more practical level, LCAs are usually manually conducted. Conducting LCAs manually is a time-consuming and error-prone endeavor: the cumbersome process of compiling inventories manually opens up for a plethora of typing errors; errors when linking processes; and when choosing materials.

In conclusion, these issues may result in LCAs that overly simplifies or in other ways misrepresent the system under scrutiny, which may in turn lead to LCA results that misleads strategic decision-making processes; and it might become impossible to generate sufficient environmental insights to improve process development (Cerdas, 2020).

Engineering models, in this case process models, on the other hand, often do not keep track of production aspects of relevance for LCA, such as composition of electrolytes (i.e., how much material is used in 100g of electrolytes).

These shortcomings call for new tools and methodologies that integrate LCA within engineering activities in a way that minimizes the trade-offs between quality, robustness, and resolution of the analyses on one hand, and applicability and uptake in the industry on the other hand (as argued by f.ex. Cerdas, 2020, p. 173).

There are several benefits of having a scripted model for this type of work. Firstly, building a modular framework gives the benefits of scalability and

extensibility, allowing the flexibility needed for product development and process optimization in the rapidly evolving field of EV battery production. When the model is coded, the code can be expanded upon with small scripts. This makes it easier to update the model with new knowledge, benchmarks and values, keeping up with the state of art. Secondly, the scripted model allows for the handling of uncertainty and variability inherent in EV battery production. Providing the possibility of generating inventories with minor changes, thus overcoming one of the main obstacles of the commonly applied Monte Carlo simulation – a sensitivity analysis that needs many runs to calculate variance (Groen et al., 2014). Thirdly, the scripted model limits human errors and the resource-intensiveness of conducting LCAs.

4 Model development

This chapter is dedicated to presenting the Coupled Battery Production and LCI Model (CBPLM) and describe how it has been developed in practice. In the first part of this chapter, a synthesis of needs, objectives and requirements for the model is given. Then, the model is presented, first with a graphical overview, then with descriptions of inputs and choice of chemistry; material data and energy data. Further, software used to develop the model is described, before moving on to a more detailed description of the development of the CBPLM. This includes how the collection and processing of input data was handled, how the foreground was structured, what user choices are available and how the various choices the user can make was implemented, and finally, how the background was structured and what its structure is dependent on. The last subchapter provides an example of the model applications.

4.1 Synthesis of needs, objectives and requirements

As concluded in chapter 3.2, there is currently a need for integrating LCA and engineering models in order to improve the decision-making processes and engineering activities in the field of battery production, along with locating sources of emissions in the production line. The objective for this thesis is thus to develop a coupled model that semi-automatically produces LCIs based upon inputs from a battery-production process model and a set of user choices, and for these LCIs to be readily assessable for the Excel- and MATLAB-based LCA software Arda.

The overall goal and scope of the model can be synthesized as follows:

- The aim with the model is for it to produce an LCI for a battery production process, populated with data from an external source on

material mass and the energy consumption of given process steps, structured in a specific way, and certain user inputs.

The requirements of the coupled model can be synthesized as follows:

- The model should be able to edit values in the LCI and produce an .xlsx file format that can be analyzed using Arda.
- There should be a way to choose which positive active material and electricity mix to be used, and the model should be able to make alterations depending on the user's choices for both of these.
- The model should be able to recalculate the input-output and process values given in a prespecified format to match the format of the LCI.
- The model should be able to alter the energy consumption and material masses depending on which battery chemistry is chosen.
- The model should be able to generate the file and the necessary sheets and save the file with either a predefined filename or a filename of the user's choice.

4.2 Presentation of the coupled model

In this sub-chapter, the CBPLM is presented, and its various components are described. Figure 6 provides a graphical overview of the coupled model.

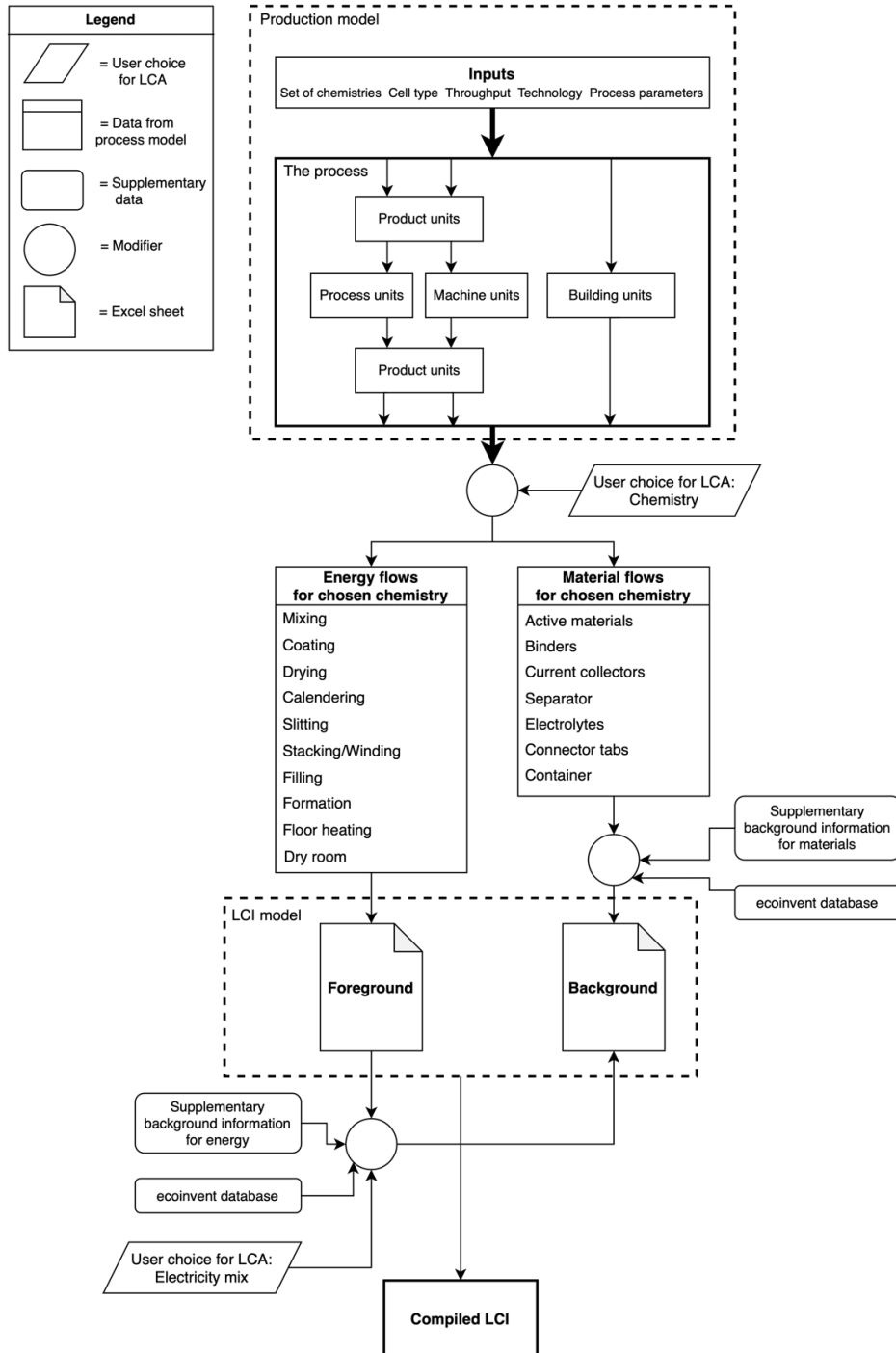


Figure 6 Coupled battery production and LCI model. The production model is adapted from Jinasena et al. (2021), while the LCI model is based upon a generic template.

First, a quick summary of the battery-production process model (see chapter 2 for a further explanation): the model accepts five different types of inputs, and through engineering modelling delivers two types of outputs. The process model is structured around four different unit types: product units, process units, machine units and building units. These unit types have different tasks. While some keeps track of either the material throughput or energy use for the process steps, the others take the machine specifications into account and calculates energy use for a special areas or rooms depending on parameters such as target humidity, temperature, or floor area.

Inputs and choice of chemistry

To begin with, the engineer chooses the inputs to the production model. For more details on the inputs, see table 1–3 below. Based on the inputs, the production model generates outputs in the form of numerical values for the energy consumption for each of the processes modelled, and the throughput of material from start to finish. At this point, the practitioner will be prompted to make a choice for which battery-cell chemistry to use in the LCA. The required user inputs specific to the LCA, will not affect the inputs to the production model. However, the LCA specific user input for the chemistry is dependent on the production model in the way that the chemistry chosen must be in the set of chemistries used as an input to the production model. It is currently possible to choose between seven different combinations of the battery anode and cathode chemistries, with three more options being available in the code but inactive due to a lack of supplementary background data and/or was unavailable in the ecoinvent database at the time of writing. The various combinations of anode and cathode chemistries are shown in Table 1.

Table 1 The ten different combinations of cathode and anode active materials modelled by the process model, of which seven are active in the CBPLM. Inactive combinations are marked with an asterix.

Cathode active material	Anode active material
LMO	Graphite/Hard carbon
NMC811	Graphite/Hard carbon
LFP	Graphite/Hard carbon
NCA	Graphite/Hard carbon
NMC622	Graphite/Hard carbon
NMC111	Graphite/Hard carbon
NMC532 (50%) and LMO (50%)	Graphite/Hard carbon
NMC532	Graphite/Hard carbon
LMO*	LTO*
NMC333	Si

Once the choice has been made, the coupled model will extract the energy and material data from the set of chemistries represented in the output files from the production model. A more detailed description of the material data and energy data from the process model that is used in the CBPLM are given in the next paragraphs.

Material data

The material mass information is given as three different values, namely as cell, base and base-scrap. The cell value yields the mass of the components in the final cell. These are commonly categorized components in a cell such as active material, carbon, binder, etc. The base and base-scrap materials are further categorizations of the cell materials into battery grade materials such as SBR and PVDF (in binder), aluminum and plastic types in cell container,

etc. Also, the solvent types and amounts that were used for making the cell is available in here. The total amount of material that goes into making the cell is the sum of the base and base-scrap values, which are given with a slightly higher resolution than the cell values. An example of the components that the outputs yield numerical information about is given in Table 2, with the main components listed on the left side of the table, with a higher resolution on the right side of the table. If the component either has alternatives to what material is used or if it requires a combination of materials, these are marked with an indent and a dash in front.

Table 2 Overview of the cell components contained in the dataset.

Cell component	Subcomponents
Anode	Active material <ul style="list-style-type: none"> - Graphite - Silicon nano-wire
	Carbon black
	Binder <ul style="list-style-type: none"> - SBR/CMC - PVDF
	Solvent <ul style="list-style-type: none"> - NMP - Water
	Current collector
Cathode	Active material
	Carbon black
	Binder

	- SBR/CMC
	- PVDF
	Solvent
Container	Current collector
	Pouch
	- Aluminum
	- Plastic PP
	- Plastic PET
	Positive terminal
	Negative terminal
Electrolyte (LiFP6, EC, DMC/EMC)	
Separator	

Energy data

For the energy inputs, a collection of the energy-consuming process steps and which component they are associated with in the CBPLM is given in table 3, while the different cathode and anode active material combinations that the battery-production process model produces outputs for are listed in table 1.

Table 3 Process steps accounted for in the LCI (right side) and the associated main components (left side).

Component	Process step
Anode	Mixing
	Coating
	Drying
	Calendering

	Slitting
Cathode	Mixing
	Coating
	Drying
	Calendering
	Slitting
Cell	Stacking/Winding
	Filling
	Formation
	Floor heating
	Dry room

From here, the absolute energy consumed in the processes themselves are inserted into the correct cells of the Foreground sheet of the LCI, which has already been generated based upon a generic LCI template. Parallel to this, the material flows for the chosen chemistry, together with supplementary information from Ellingsen et al. (2014) on the necessary background processes and production facilities associated with the materials in question, and data from the ecoinvent database, are placed in the correct format in the Background sheet of the LCI. Not shown in the figure, are some necessary conversions of the units used in the production model's outputs, for both the energy and material data, to units matching those of the ecoinvent 3.2 database.

Further, the energy amounts from the Foreground sheet are coupled with the ecoinvent database, along with supplementary data from Ellingsen et al.

(2014) with factors accounting for the losses in the electrical grid, length of various types of electrical grid needed, and a very climate-potent material associated with electricity production.

At this point, the user will get another prompt, this time to somewhat account for the spatial variability in terms of GWP when producing a battery, as this is something that can affect the type and amounts of emissions substantially. To somewhat account for the this, the user must choose which electricity mix to be simulated in the LCI of the battery production. The global warming potential impacts related to the production of battery cells are highly dependent on the country they are produced in, as different countries' sources of electricity production vary. Therefore, by allowing the user to choose the electricity mix, one can compare how changing the geographical location affects the impacts of the battery production. In the background tab of the LCI, the total amount of electricity used for a process is being read from the foreground section, before it is multiplied with the shares of the different electricity producing sources in the selected electricity mix. Further, it is multiplied with two factors to account for unavoidable losses such as losses associated with energy transfer in the transmission network.

Once an electricity mix has been chosen, the data are inserted in the Background sheet in the correct format and structure. At this point, the compiled LCI has been populated with all the necessary data and is in a format accepted by the Arda software.

4.3 Software

This section briefly describes which software was used to create the CBPLM, and which software is required to use the model.

The model consists of a Python (3.9.2) based interface which connects an LCA model with a Python (3.7) based cell production model in order to produce Excel files that are accepted by the LCA software Arda.

Here, Python is used (with the `openpyxl` module, an open-source Python library for reading and writing Excel) to fetch, structure and save data in Excel and to run Arda through MATLAB. The Python based cell production model from which I'm compiling the inventories needed in the Python file, is derived from Jensina et al (2021). My end result is Excel file(s) that is read by Arda through MATLAB to calculate the results of the LCI using the ecoinvent 3.2 database, which was released in December 2020.

As there are some issues with the MATLAB packages in Python, it is not possible to do this coupling in every Python version. To run MATLAB through Python, you need compatible versions of Python. This step therefore had to be truncated.

In order to run the model, the user needs a virtual Python environment with the `openpyxl` module installed, and to run an impact assessment in Arda, the user needs access to MATLAB.

4.4 Development of the coupled model

The following subchapter explains the technical development of the coupled model, i.e., the programming.

Collection of input-output and process data

The model is capable of using data from either a .CSV or .xlsx file as long as they are arranged in the correct way, as the same way as the file shown in the digital appendix. The LCI has been developed by using data from Jinasena et al. (2021) and supplemented with data from Ellingsen et al. (2014).

Processing input-output and process data

If the data source for the input data is in an .xlsx format, it can be directly recalculated and used to fill in the correct cells in the LCI, using the Python library openpyxl. If, however, the data source for the input data is in a .CSV format, it must first be read using the Python csv module, before using the openpyxl library to recalculate the values to their correct format, before using the values as input to the correct LCI cells. The name of the battery chemistry, along with the corresponding values are scanned, extracted and being structured based on the chemistry and type of value.

Building foreground based on template

The foreground is modelled after a template, and the main processes and components have been accounted for. First, the template itself, containing generic headlines and names which are not reliant on any external information, is coded in. Next, a variable containing the names of the main components and processes which are equal for all the battery types is created, named foreground_names. Then, a variable called battery_chemistries is generated, containing all the different names of the various positive electrode materials

that is currently accounted for. Both of the variables can be expanded/alterd quite easily by going to the “Foreground” section in the code and add/alter values in the two variables mentioned above. The foreground sections FULL NAME and NAME will, by the use of a for-loop and some if-conditions, be implemented, first by looping through and inserting the names in the foreground_names variable, and then by looping through and inserting the names in the battery_chemistries variable.

Due to time constraints, some of the more absolute values such as the functional unit and the interdependencies between the main components, excluding the positive electrode active materials, have been programmed in such a way that they won't change automatically if new processes/components are added. These can however easily be changed manually in the “Foreground” section to adapt the script to alterations. The energy use for the various process steps, which will be dependent on the battery chemistry in question, will be read from an external file with the correct format of the practitioner's choice, and the energy values will be added to the correct cells after having been recalculated to a kWh format as described above. Only one of the positive electrode chemistries will be active at one time, chosen by the practitioner through an input query upon running the script. The chosen cathode material will receive a '1' in the cell in the positive active material-column on the 2nd row.

Both the foreground and background process code have been color coded to improve readability.

Importing and programming values for electricity mix

The electricity mix is based on data from IEA for data from 2019 (IEA, 2020a). First, a sheet named Electricity_mixes is generated using the openpyxl library. Next, the names of the various countries and electricity sources are filled in in a table format. As the electricity mix values in IEA's dataset is in absolute values (GWh), they have first been recalculated to percentage shares before being programmed in to excel in their respective cells. These values are later used in the background (A_bf), depending on the electricity mix chosen by the practitioner, as will be discussed further in the next section/subchapter.

Building background based on foreground and data

The background section is the largest and most complex part of the program, partly due to the sheer amount of information required. To begin with, variables containing necessary information, mostly Arda IDs for all the different processes, along with the generic template structure of the background are created. These variables, in addition to being used to populate the respective cells in the (Arda ID) column, are also used to decide the number of rows in the background sheet. In addition, by populating the cells in the A and F columns with the VLOOKUP function in Excel, using the Arda IDs in the C column as the lookup-value, the name and units of the corresponding processes are extracted directly from the PRO sheet in the LCI in the A and F columns respectively. To populate the E column, there are three ways the data is being generated. The first way is from the data gathered in the collection input-output and process data, either directly or after having been recalculated to fit the format of the LCI. The second way is where data is dependent on other values i.e., for the electricity mix, the energy use in kWh is being distributed between the energy production processes based on the shares of the selected electricity mix. The third and final way is data, which in this case is gathered from Ellingsen et al. (2014), to make up for the pieces of

missing information in the collection-of-data phase. For the latter, at the moment of programming and writing data for these background processes/materials were not available, and data from a different source was used to make up for that. For the electricity mix, the practitioner will get an input query upon running the script requesting which countries electricity mix is to be used. The various shares of the electricity mix will then change depending on the country chosen, and the name of the country will be displayed above the names of the energy production technologies. Further, the values in the E column for all the energy demanding process steps will be calculated based on the chosen electricity mix and the absolute energy value for the respective process steps in the foreground sheet.

4.5 Model example applications

This chapter is dedicated to give an example of the results obtained by using the coupled model and to compare these with some reference values from literature. A breakdown of the values produced by the coupled model for one of the chemistries and a given electricity mix will then be presented to show the distribution of GWP impacts caused by the production of that particular cell using the chosen electricity mix.

Figure 7 showcases reference values for GHG emissions for two battery cells from literature, namely an NMC cell from Ellingsen et al. (2014) and a combined LMO and NMC cell from Kim et al. (2016). Further, it compares these reference values to values generated by the coupled model, using data from the process model of Jinasena et al. (2021).

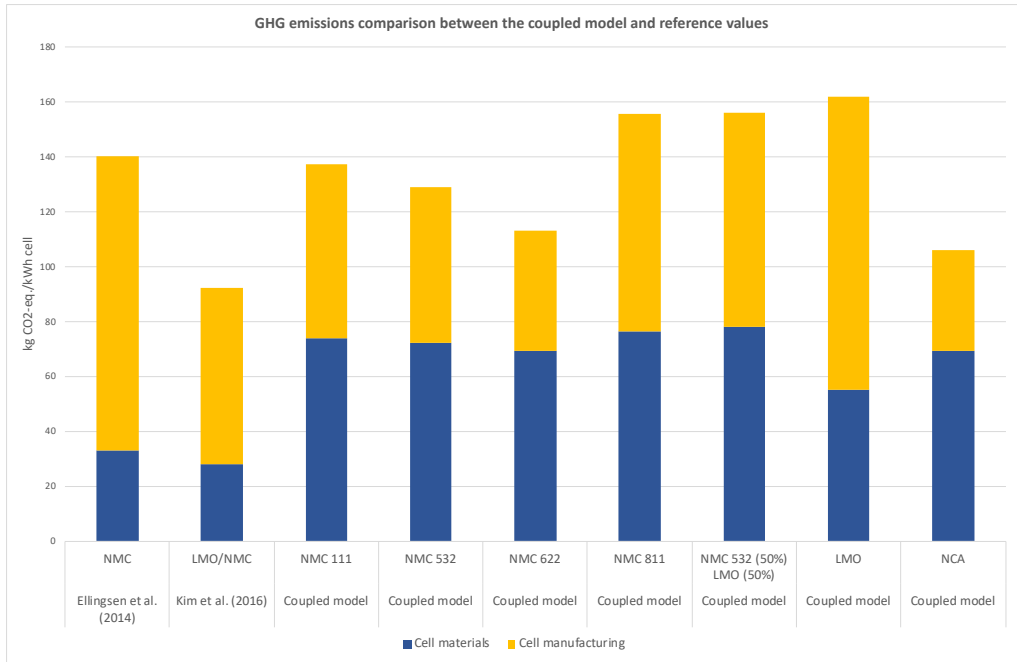


Figure 7 Comparison of example data for GHG emissions from the coupled model with reference data from literature

Further, one can see that the GHG emissions attributed to the cell materials are much greater for all the coupled model cells than for the two cells from literature. This is likely to stem from a difference in materials included, the composition of these and how the material shares between primary and recycled materials differ between the coupled model and the reference literature. In the coupled model, an assumption of no recycled material was made, while Ellingsen et al. (2014) and Kim et al. (2016) both assume portions of the material to be recycled, which would lower the GWP impact of the cell materials. Other differences between the datasets can also be caused by the fact that the reference data are from 2014 and 2016, which can be a factor as the ecoinvent version used has changed, which can cause differences in the carbon footprint of the energy generation technologies, and that the battery production technology has improved since the reference literature studies were published. Another source of difference can be the input data, and the

increased resolution of the coupled model, which is made clear by the breakdowns of GHG emissions in Table 4 and Table 5, which allows for a better understanding of the source of the GHG emissions as the level of detail is increased, especially for the manufacturing processes. The cell used as an example in Table 4 and Table 5 is an NMC 811 cell.

Table 4 Breakdown of CO₂ emissions due to the cell materials

GWP of cell materials				
Component	Subcomponent	kg CO ₂ -eq./kWh	Share of GWP (%)	
Battery cell	-	0,21	0,27%	0,27%
Anode	Negative current collector	3,78	4,97%	9,23%
	Negative electrode paste	0,76	1,00%	
	Negative active material	2,25	2,96%	
	Negative binder	0,24	0,31%	
Cathode	Positive current collector	5,50	7,22%	81,37%
	Positive electrode paste	13,77	18,09%	
	Positive binder	0,87	1,14%	
	NMC811-G	7,50	9,85%	
	Precursor NCM	5,17	6,79%	
	Cobalt sulphate	29,13	38,27%	
Container	Pouch	1,51	1,98%	4,71%
	Anode tab	1,06	1,39%	
	Cathode tab	1,02	1,34%	
Electrolyte	-	3,17	4,17%	4,17%
Separator	-	0,19	0,24%	0,24%
Total		76,12	100%	100%

Table 4 shows a breakdown of the GWP impacts for the cell materials. This breakdown shows that the cathode materials are responsible for the majority of the GHG emissions stemming from material usage (81,37 %), and that the cobalt sulphate and the other components for the positive electrode paste make up about 56 % of the cathode material's GHG emissions.

In Table 5, a breakdown of the GHG emissions for the manufacturing processes required for the cell is given. Out of all the energy consuming processes, the dry room is responsible for over half the GWP impacts. Another major contributor to the GWP impacts is the drying of the cathode, responsible for almost 37 % of the manufacturing processes' GHG emissions, which is almost four times as great as for the drying of the anode. The manufacturing processes make up 51 % of the cell's total GHG emission, while the materials are responsible for the remaining 49 %.

Table 5 Breakdown of CO2 emissions due to the direct energy use of the cell production processes

GWP of cell manufacturing processes			
Component	Process step	kg CO₂-eq./kWh	Share of GWP (%)
Anode	Mixing	0,00	0,00%
	Coating	0,00	0,00%
	Drying	7,88	9,94%
	Calendering	0,00	0,00%
	Slitting	0,00	0,00%
Cathode	Mixing	0,00	0,00%
	Coating	0,00	0,00%
	Drying	30,68	38,67%
	Calendering	0,00	0,00%
	Slitting	0,00	0,00%
Cell	Stacking/Winding	0,00	0,00%
	Filling	0,00	0,00%
	Formation	0,15	0,19%
	Floor heating	0,00	0,00%
	Dry room	40,63	51,21%
Total		79,33	100%

5 Limitations and further work

5.1 Limitations

The lack of availability of primary data for the battery production limits the quality of the LCI, as some of the data can be outdated or only viable for smaller production scales. Further, there were significant gaps between the available data from the process model and the background data necessary to keep a high resolution. Preferably, this data would all come from one, primary source, instead of using supplementary data from other sources. In addition, the data could be crosschecked against more sources to validate its results further, which was not possible for this thesis due to time constraints.

5.2 Further work

There exist numerous possibilities for how to expand and further develop the coupled model, for the most part only limited by imagination, as new blocks of code can easily be added. A natural way to progress, would be to attempt to integrate the coupled model more into the process model so that one could get more direct results and the ability to only look at parts of the production chain. Further, a simple user interface would increase the user friendliness of the coupled model, and thus maybe making it more tempting to use in both industry and academia. Parts of the code could also be made more flexible to make it easier to use in combination with other process models.

References

- Bryntesen, S. N., Strømman, A. H., Tolstorebrov, I., Shearing, P. R., Lamb, J. J., & Stokke Burheim, O. (2021). Opportunities for the State-of-the-Art Production of LIB Electrodes—A Review. *Energies*, *14*(5), 1406. <https://www.mdpi.com/1996-1073/14/5/1406>
- Cerdas, F., Thiede, S., & Herrmann, C. (2018). Integrated Computational Life Cycle Engineering — Application to the case of electric vehicles. *CIRP Annals*, *67*(1), 25-28. <https://doi.org/https://doi.org/10.1016/j.cirp.2018.04.052>
- Cerdas, F., Titscher, P., Bognar, N., Schmuch, R., Winter, M., Kwade, A., & Herrmann, C. (2018). Exploring the Effect of Increased Energy Density on the Environmental Impacts of Traction Batteries: A Comparison of Energy Optimized Lithium-Ion and Lithium-Sulfur Batteries for Mobility Applications. *Energies*, *11*(1), 150. <https://www.mdpi.com/1996-1073/11/1/150>
- Cerdas, J. F. (2020). *Integrated Computational Life Cycle Engineering for Traction Batteries* [Doctoral dissertation, Technischen Universität Braunschweig]. Fakultät für Maschinenbau.
- Dai, Q., Kelly, J. C., Gaines, L., & Wang, M. (2019). Life Cycle Analysis of Lithium-Ion Batteries for Automotive Applications. *Batteries*, *5*(2), 48. <https://www.mdpi.com/2313-0105/5/2/48>
- Dunn, J. B., Gaines, L., Kelly, J. C., James, C., & Gallagher, K. G. (2015). The significance of Li-ion batteries in electric vehicle life-cycle energy and emissions and recycling's role in its reduction [10.1039/C4EE03029J]. *Energy & Environmental Science*, *8*(1), 158-168. <https://doi.org/10.1039/C4EE03029J>
- Ellingsen, L. A.-W., Hung, C. R., & Strømman, A. H. (2017). Identifying key assumptions and differences in life cycle assessment studies of lithium-ion traction batteries with focus on greenhouse gas emissions. *Transportation Research Part D: Transport and Environment*, *55*, 82-90. <https://doi.org/https://doi.org/10.1016/j.trd.2017.06.028>
- Ellingsen, L. A.-W., Majeau-Bettez, G., Singh, B., Srivastava, A. K., Valøen, L. O., & Strømman, A. H. (2014). Life Cycle Assessment of a Lithium-Ion Battery Vehicle Pack. *Journal of Industrial Ecology*, *18*(1), 113-124. <https://doi.org/https://doi.org/10.1111/jiec.12072>

- Groen, E., Heijungs, R., Bokkers, E. A. M., & Boer, I. J. M. (2014). *Sensitivity analysis in life cycle assessment*.
- Hauschild, M. Z., Goedkoop, M., Guinée, J., Heijungs, R., Huijbregts, M., Jolliet, O., Margni, M., De Schryver, A., Humbert, S., Laurent, A., Sala, S., & Pant, R. (2013). Identifying best existing practice for characterization modeling in life cycle impact assessment. *The International Journal of Life Cycle Assessment*, 18(3), 683-697. <https://doi.org/10.1007/s11367-012-0489-5>
- Hauschild, M. Z., Rosenbaum, R. K., & Olsen, S. I. (2018). Life Cycle Assessment : Theory and Practice. <https://doi.org/10.1007/978-3-319-56475-3>
- Hawkins, T. R., Singh, B., Majeau-Bettez, G., & Strømman, A. H. (2013). Comparative Environmental Life Cycle Assessment of Conventional and Electric Vehicles. *Journal of Industrial Ecology*, 17(1), 53-64. <https://doi.org/https://doi.org/10.1111/j.1530-9290.2012.00532.x>
- Herrmann, C., & Thiede, S. (2009). Process chain simulation to foster energy efficiency in manufacturing. *CIRP Journal of Manufacturing Science and Technology*, 1(4), 221-229. <https://doi.org/https://doi.org/10.1016/j.cirpj.2009.06.005>
- IEA. (2020a). *Electricity Information: Overview*. <https://www.iea.org/reports/electricity-information-overview>
- IEA. (2020b). *Global EV Outlook 2020*. <https://doi.org/https://doi.org/10.1787/d394399e-en>
- IEA. (2020c). *Tracking Transport 2020*. <https://www.iea.org/reports/tracking-transport-2020>
- Jinasena, A., Burheim, O. S., & Strømman, A. H. (2021). A Flexible Model for Benchmarking the Energy Usage of Automotive Lithium-Ion Battery Cell Manufacturing. *Batteries*, 7(1), 14. <https://www.mdpi.com/2313-0105/7/1/14>
- Johansen, D. A. (2020). *Expanding the Life Cycle Inventory for production of Li-ion NMC pouch cells by introducing processes to increase resolution of production impacts* [Energy and Environment, Specialization Project (student paper)]. NTNU.
- Kim, H. C., Wallington, T. J., Arsenault, R., Bae, C., Ahn, S., & Lee, J. (2016). Cradle-to-Gate Emissions from a Commercial Electric Vehicle Li-Ion Battery: A Comparative Analysis. *Environmental Science & Technology*, 50(14), 7715-7722. <https://doi.org/10.1021/acs.est.6b00830>

- Kurland, S. D. (2019). Energy use for GWh-scale lithium-ion battery production. *Environmental Research Communications*, 2(1), 012001. <https://doi.org/10.1088/2515-7620/ab5e1e>
- Mayer, J. K., Almar, L., Asylbekov, E., Haselrieder, W., Kwade, A., Weber, A., & Nirschl, H. (2020). Influence of the Carbon Black Dispersing Process on the Microstructure and Performance of Li-Ion Battery Cathodes. *Energy Technology*, 8(2), 1900161. <https://doi.org/https://doi.org/10.1002/ente.201900161>
- Meyer, C., Kosfeld, M., Haselrieder, W., & Kwade, A. (2018). Process modeling of the electrode calendaring of lithium-ion batteries regarding variation of cathode active materials and mass loadings. *Journal of Energy Storage*, 18, 371-379. <https://doi.org/https://doi.org/10.1016/j.est.2018.05.018>
- Nealer, R., & Hendrickson, T. (2015). Review of Recent Lifecycle Assessments of Energy and Greenhouse Gas Emissions for Electric Vehicles. *Current Sustainable/Renewable Energy Reports*, 2. <https://doi.org/10.1007/s40518-015-0033-x>
- Notter, D. A., Gauch, M., Widmer, R., Wäger, P., Stamp, A., Zah, R., & Althaus, H.-J. (2010). Contribution of Li-Ion Batteries to the Environmental Impact of Electric Vehicles. *Environmental Science & Technology*, 44(17), 6550-6556. <https://doi.org/10.1021/es903729a>
- Ouellet-Plamondon, C., & Habert, G. (2015). 25 - Life cycle assessment (LCA) of alkali-activated cements and concretes. In (pp. 663-686). <https://doi.org/10.1533/9781782422884.5.663>
- Pettinger, K.-H., & Dong, W. (2016). When Does the Operation of a Battery Become Environmentally Positive? *Journal of the Electrochemical Society*, 164(1), A6274-A6277. <https://doi.org/10.1149/2.0401701jes>
- Schmitt, J., Raatz, A., Dietrich, F., Dröder, K., & Hesselbach, J. (2014). Process and performance optimization by selective assembly of battery electrodes. *CIRP Annals*, 63(1), 9-12. <https://doi.org/https://doi.org/10.1016/j.cirp.2014.03.018>
- Schreiner, D., Oguntke, M., Günther, T., & Reinhart, G. (2019). Modelling of the Calendaring Process of NMC-622 Cathodes in Battery Production Analyzing Machine/Material–Process–Structure Correlations. *Energy Technology*, 7(11), 1900840. <https://doi.org/https://doi.org/10.1002/ente.201900840>
- Schünemann, J. H. (2015). *Modell zur Bewertung der Herstellkosten von Lithiumionenbatteriezellen* (Vol. 1). Sierke.

- Schönemann, M., Bockholt, H., Thiede, S., Kwade, A., & Herrmann, C. (2019). Multiscale simulation approach for production systems. *The International Journal of Advanced Manufacturing Technology*, 102(5), 1373-1390. <https://doi.org/10.1007/s00170-018-3054-y>
- Sun, X., Luo, X., Zhang, Z., Meng, F., & Yang, J. (2020). Life cycle assessment of lithium nickel cobalt manganese oxide (NCM) batteries for electric passenger vehicles. *Journal of Cleaner Production*, 273, 123006. <https://doi.org/https://doi.org/10.1016/j.jclepro.2020.123006>
- The International Standards Organisation. (2006). Environmental management — Life cycle assessment — Principles and framework. *BMJ*, 332. <https://doi.org/10.1136/bmj.332.7550.1107>
- Thomitzek, M., Schmidt, O., Röder, F., Krewer, U., Herrmann, C., & Thiede, S. (2018). Simulating Process-Product Interdependencies in Battery Production Systems. *Procedia CIRP*, 72, 346-351. <https://doi.org/https://doi.org/10.1016/j.procir.2018.03.056>
- Thomitzek, M., von Drachenfels, N., Cerdas, F., Herrmann, C., & Thiede, S. (2019). Simulation-based assessment of the energy demand in battery cell manufacturing. *Procedia CIRP*, 80, 126-131. <https://doi.org/https://doi.org/10.1016/j.procir.2019.01.097>
- Volkswagen. (2012). *The e-mission. Electric Mobility and the Environment*. https://www.volkswagenag.com/presence/nachhaltigkeit/documents/the_e-mission.pdf
- Yuan, C., Deng, Y., Li, T., & Yang, F. (2017). Manufacturing energy analysis of lithium ion battery pack for electric vehicles. *CIRP Annals*, 66(1), 53-56. <https://doi.org/https://doi.org/10.1016/j.cirp.2017.04.109>

Digital appendix

The code and files used in developing the coupled model are available at:

<https://github.com/DanAndreJohansen/Master-project-A-coupled-battery-production-and-LCI-model>

